Case Reports in Neurology

Case Rep Neurol 2023;15:177–186
DOI: 10.1159/000530980
Received: December 13, 2022
Accepted: May 2, 2023
Published online: May 26, 2023

Case Report

Utilizing Reduced Labeled Proton Clearance to Identify Preclinical Alzheimer Disease with 3D ASL MRI

Charles R. Joseph[a] Alec Kreilach[b] Victoria Ashley Reyna[b] Thomas Ashton Kepler[b] Brittany Viola Taylor[b] Jubin Kang[b] Dallas McCorkle[b] Nicholas L. Rider[c]

[a]Department of Neurology, Liberty University College of Osteopathic Medicine (LUCOM) Lynchburg, VA, USA; [b]LUCOM medical student, Lynchburg, VA, USA; [c]Department of Bioinformatics and Immunology, LUCOM, Lynchburg, VA, USA

Keywords
Glymphatic clearance · Arterial spin labeling MRI · Preclinical Alzheimer disease · Capillary mean transit time · Blood-brain barrier leak

Abstract
Addressing the seminal pathophysiology in Alzheimer disease (AD) is the next logical focus for effective intervention, given the initial disappointing and more recent possibly encouraging results of monoclonal antibody trials. Endothelial cell dysfunction-induced blood-brain barrier leak with associated prolonged capillary mean transit time (cMTT) and glymphatic outflow dysfunction is the most proximal events in the degeneration cascade. Sensitive and reproducible markers are required to both identify early disease and assess future treatment trial outcomes. Two participants, with mild cognitive impairment (MCI) and one with AD, were evaluated clinically prior to MRI in this small case series report. From seven 3D turbo gradient and spin echo (TGSE) pulsed arterial spin echo (PASL) MRI sequences six homologous region of interest in bitemporal, bifrontal, and biparietal lobes for each sequence were examined and plotted against time. By choosing late perfusion times during cMTT phase of perfusion linear analysis of signal decay could be utilized. A reference axial FLAIR sequence was also obtained. Slope of the linear analysis correlated to the rate of labeled proton clearance with reduced clearance occurring in AD participants compared to normal participants in our previous study. Whether similar differences in clearance rate extend to either MCI or early AD was investigated. Participants were categorized by clinical phenotype before MRI and compared to previously published phenotype cohorts: n = 18 normal/healthy, n = 6 AD, n = 3 MCI. Significant differences in labeled proton clearance rates between AD and MCI/control phenotypes within bilateral temporal lobes (left p = 0.004, right p = 0.002) and

Correspondence to:
Charles R. Joseph, crjoseph@liberty.edu

Case Rep Neurol 2023;15:177–186
DOI: 10.1159/000530980

within bilateral frontal lobes AD versus controls (left p = 0.001, right p = 0.008) and AD versus MCI (left p = 0.001, right p = 0.001) were found. This noninvasive MRI technique has potential for identifying MCI transition to AD.

Introduction

Given the encouraging results of the Lecanemab treatment trial targeting β-amyloid and pTau in clinically apparent Alzheimer's disease (AD) due to presence of irreversible damage, the focus of intervention is shifting to earlier treatment of upstream pathologic changes. The sentinel events occur years prior to accumulation of misfolded proteins associated with mild cognitive impairment (MCI) or without symptoms [1, 2]. Early identification of AD requires screening for those with associated health risks and employing sensitive biologic/pathologic markers of the early phases of disease. The earliest identifiable event thus far described is breakdown of the blood-brain barrier (BBB) by microglia immune targeting via expression of complement C3a of endothelial cells (ECs) [1, 3]. Inflammatory signaling of microglia triggers its release of C3a (complement) resulting in EC morphologic shift to immunocompetent cells as EC cell surface C3aR (receptors) are upregulated causing retraction of EC walls via activation of cytoskeletal myosin opening tight junctions [1]. They also express vascular cell adherent molecules (VCAM 1) on the EC surface attracting lymphocytes [1–7]. The inflammatory response within the interstitial space is muted in comparison to incitement by infection [1, 3]. Further, pericapillary pericytes are damaged early as a consequence of the inflammatory response altering autoregulatory blood flow [5–7]. The functional changes in the ECs causing BBB leak, prolong the normal capillary mean transit times (cMTT) as the capillary autoregulatory system fails [7]. A recent study has demonstrated the BBB leak of only small molecules in AD as opposed to large molecular leak in vascular-related dementia [8, 9]. The BBB leak of damage-associated molecular patterns, pathogen-associated molecular patterns, and inflammatory cells into the interstitium disrupts both normal metabolic processes within the neuropil and the glymphatic system through early pericyte loss, causing impairment of interstitial waste clearance in advance of plaque and tangle formation [10–12]. Recent discoveries have demonstrated proteinaceous connections between capillary pericytes and/or fibrocytes with the astrocyte aquaporin channels across the glymphatic space separating the two [13]. Disruption of these connections early in BBB breakdown process from pericyte damage contributes to the early disruption of the glymphatic system. The subsequent inflammatory and toxin accumulation alters normal metabolic processes leading to downstream misfolding, accumulation, and dispersion of first β-amyloid and later hpTau. Both misfolded proteins accelerate the BBB leak, and as the process worsens, ultimately causes neuronal cell death [10–12]. With evidence of small molecule BBB leak in AD, arterial spin labeled (MRI) water in blood may serve as an excellent marker of impaired perfusion outflow. Whether its accumulation is related to primarily dysfunction of the glymphatic system or to prolonged cMTT is less important than leveraging delayed clearance measurement as a physiologic tool for early identification of BBB leak in preclinical AD. As potential therapeutic targets for clinical trials are developed to mitigate AD before the neurodegenerative cascade ensues; simple, readily available, noninvasive, and reproducible outcome measures must be available [14].

MRI tools for preclinical AD diagnosis fall into 3 general categories: subtle anatomic alterations identified using machine learning, accumulation of aberrant proteins using

spectroscopy, and demonstration of pathophysiologic leak of contrast agents or alterations in perfusion [14, 15]. Pulsed arterial spin labeling (PASL) MRI is a fast, inexpensive, and noninvasive method of investigating perfusion when compared to high-resolution dynamic contrast enhanced MRI. It employs a proton labeling pulse in the neck and measures its signal within the brain after a time delay (TI) with background signal suppression [16, 17]. The residual signal is from the remaining labeled intracapillary blood protons and those leaked into interstitial spaces. We used long TI times thereby minimizing arterial contribution, thus allowing for linear analysis (Fig. 1) [18, 19]. The region of interest (ROI) in each of the homologous brain regions avoided ventricular or subarachnoid spaces in the chosen areas of interest [18]. The method described below has identified reduced labeled proton signal clearance over time in AD patients compared to normal in three bilateral brain regions [16, 18]. Here, we present a small case series of participants at earlier stages of dementia expanding on previous published work utilizing 3D TGSE PASL [18].

Case Series Presentation

The CARE Checklist has been completed by the authors for this case report, attached as online supplementary material (for all online suppl. material, see https://doi.org/10.1159/000530980). After informed written consent was obtained, three unpaid volunteers were studied, two with MCI (one 65-year-old male, one 76-year-old female) and one participant (70-year-old male) with established AD diagnosis on clinical grounds by other examiners. Initial health screening (excluding individuals with potentially confounding comorbidities such as long-term diabetes mellitus, stroke, severe head injury history, cancer, or severe heart disease) was performed by their personal physicians and referred for ASL-MRI study. A detailed health questionnaire and MMSE (Folstein Mini-Mental Status Exam) was administered prior to the MRI study. All participants were studied in the early evening. The imaging characteristics for each participant will be presented. Participant 1 presented with amnestic MCI (but cognitively declined over ensuing year and a half) was scanned three times; initially and again 17 and 18 months later.

Participant 2 with established moderately severe AD dementia (diagnosed clinically elsewhere) was studied once. The diagnosis was confirmed at a second University center details are unavailable. MMSE score and mental status exams prior to our study showing impaired judgement and short-term memory were compatible with the diagnosis of AD.

Participant 3 with stable amnestic MCI (studied twice initially then 6 months later). The noninvasive MRI method employed 3D PASL ASL MRI using seven serial sequences with progressively longer TIs at 200 ms intervals, and a whole head axial FLAIR sequence for reference. Siemens 3T Skyra magnet with 20 channel receiver head coil was used for all data acquisitions. 3D TGSE PASL used FAIR and Q2TIPS labeling scheme in all seven data acquisitions [20–22]. The parameters utilized for all participants: FOV 250 mm × 250 mm, TE 16.36 ms (all sequences), TR 3830 with inversion time (TI) 2800; TR 4330 with TI 3000; TR 5000 with TI 3200; TR 5320 for the following TIs 3400, 3600, 3800, and 4000 (TR was modified in the later sequences to accommodate longer TI). Post-inversion image acquisition time was 350 ms. A 63 × 64 × 40 matrix was employed. Four pairs and 12 segments were acquired. Bolus labeling duration was 700 ms. with Turbo factor of 18, and EPI factor of 21. Q2TIPS and vendor-supplied proprietary background suppression were used. Bandwidth of 2,368/pixel and echo spacing of 0.57 ms were employed. Interleaved 40–4 mm image slices were obtained per sequence and voxel size was 3.9 × 3.9 × 4 mm^3. Siemens Digital Imaging and Communications in Medicine image reconstruction was transferred to McKesson PACS (picture archiving and communication system) for ROI tool analysis. Grayscale images were obtained. The elliptical manually adjustable tool supplied

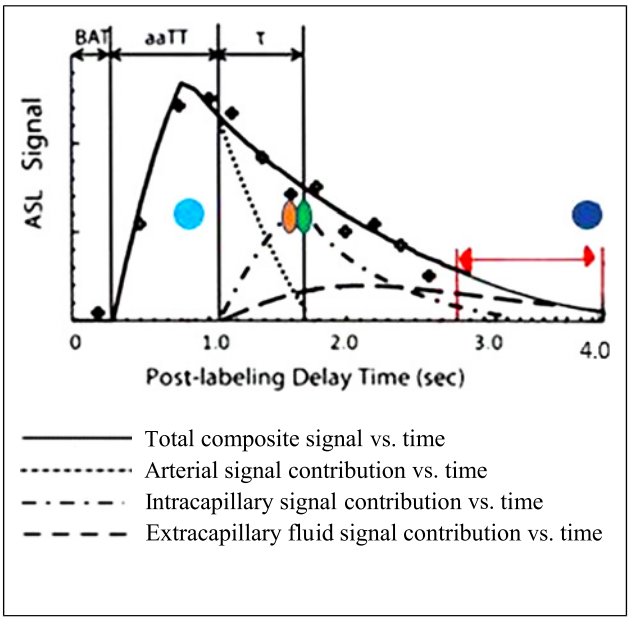

Fig. 1. Composition of the ASL signal/time into its various components: arterial, capillary, and extra-capillary spaces. TI (acquisition) times utilized in this study are between the red arrow limits. Note the signal composition is capillary and extra-capillary (interstitial) water, the latter is normally cleared by the glymphatic system. T1 times (63% signal decay) of major signal contributors indicated by the colored dots. Magenta dot = 800–850 ms T1 of white matter. Orange dot = 1,650 ms T1 of blood. Green dot = 1,700 ms T1 of gray matter (all values are for 3T). Dk blue dot = 3,800 ms T1 of water (CSF fluid) (all values are for 3T). BAT, bolus arrival time; aaTT, artery-artery arrival time; τ, peak capillary arrival time. Adapted with publisher permission (Wiley) from reference 19.

signal average, signal range, and volume studied. The total scan time for the seven sequences was about 20 min, with approximate average scan time per sequence of 2 min 15 s. After slice selection of homologous bitemporal, bi-frontal, and biparietal regions (same slice across all 7 sequences), standardized sized ROI was delineated, with signal averages recorded on a spreadsheet (Fig. 2). Subarachnoid and ventricular spaces were avoided. The long TI times allowed for best fit linear analysis [18]. The line slope indicated the rate of signal/glymphatic clearance.

Statistical Methods

Signal average for each timepoint and location was plotted, and mean slopes were calculated as clearance rates for each participant and brain region. Data for comparing clearance rates across participant phenotypes with AD (n = 6), MCI (n = 3), and control (n = 18) for each of the 6 brain regions were aggregated from this updated work and that which was previously published [18] (online suppl. Table 1). Because participant 1 initially presented clinically with MCI in 2019, ASL data from that measurement were labeled "MCI." Follow-up ASL data on participant 1 in April and May of 2021 was labeled "AD" in alignment with the noted clinical progression to AD. To compare differences across the 3 clinical phenotype categories for each brain region, one-way analysis of variance (ANOVA) was conducted (Table 1) and where significant differences were noted, a Tukey posttest was run for multiple group comparisons (Table 2). A family-wise error rate of 0.05 was used for multiple comparison testing and p values <0.05 were considered significant. Statistical analyses were done via Python v. 3.10.5, SciPy, stats and Statsmodel packages.

Discussion

In this small case series, participant 1 showed conversion from MCI clinically to early AD with pronounced decline in labeled proton clearance over the 15-month interval between studies. Participant 2 presented with both clinical and reduced clearance of AD

Case Rep Neurol 2023;15:177–186
DOI: 10.1159/000530980

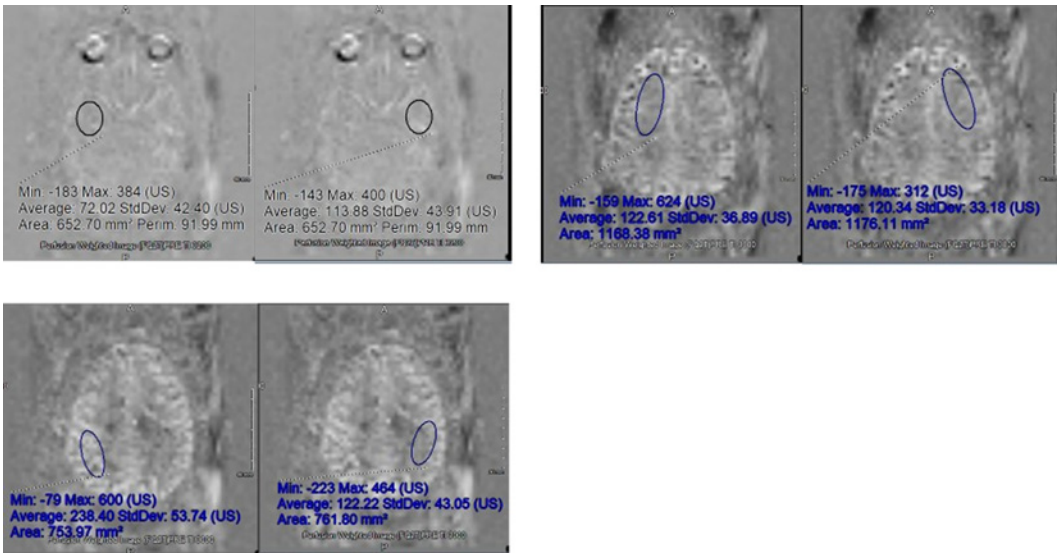

Fig. 2. Images depict the typical location of the hand-drawn region of interest (ROI) analyzed for each brain region. The area averaged in each brain region was held constant; temporal lobes 650 mm^2, frontal lobes 1,150 mm^2, and parietal lobes 760 mm^2. Subarachnoid and ventricular spaces were avoided in the ROI. Images: Top left is temporal lobe ROI, top right is frontal lobe ROI, and bottom left is parietal lobe ROI.

noted in the pilot study. Participant 3 showed no clinical decline (remains in amnestic MCI category by MMSE) but showed nonsignificant reduction in parietal lobe clearance in the 6-month interval between studies.

The mean slopes, indicative of glymphatic clearance rates within all 6 brain regions and the 3 clinical phenotypes, are shown in Table 1. From this, we note significant differences across phenotypes within bilateral temporal and frontal lobes. Table 2 shows multiple comparison testing which reveals differences between AD and control phenotype average clearance within bilateral temporal and frontal lobes. Similarly, we note differences in clearance between AD and MCI within bilateral frontal lobes. In contrast, our comparison of phenotypes within bilateral parietal lobes did not quite reach significance (p = 0.07, p = 0.07) in this study. Initial and repeated clearance slopes from the 3 newly studied participants and the associated MMSE scores are found in (Table 3).

In this study, we demonstrate the progression of MCI to early stage dementia in one participant with associated reduced rate of capillary phase of perfusion with retention or reduced clearance of labeled protons in the bitemporal and bi-frontal lobes compared to his baseline study. The changes in clearance in participant 2 of this study mirrors reduced clearance in bitemporal and bi-frontal lobes we found in AD participants in our pilot study. The retained labeled protons reflect prolonged capillary transit times and/or dysfunctional glymphatic clearance secondary to BBB leak. The connection between BBB leak and cMTT is analogous to comparing rate of water flow at low pressure between a regular garden hose and a "perforated soaker hose" (purposely designed to leak water) with flow rate and pressure considerably faster/higher in the intact regular hose. The connection of the BBB leak and glymphatic dysfunction is loss of the proteinaceous connections across the basement membranes connecting the pericytes (an early casualty of BBB leak) and the AQ 4 channels [6]. Importantly, we also note a statistically significant difference between AD and MCI phenotypes within bi-frontal lobes and a trend toward an overall difference in clearance across phenotypes within the parietal lobes (Table 1).

Case Rep Neurol 2023;15:177–186
DOI: 10.1159/000530980

Table 1. Statistical analysis of glymphatic clearance rate across brain regions

Brain region	Clinical phenotype	Mean slope	ANOVA p value (test statistic)
Left temporal lobe	AD	−0.0167	*0.006 (6.4)
	MCI	−0.0500	
	Control	−0.0583	
Right temporal lobe	AD	−0.00673	*0.002 (8.0)
	MCI	−0.0625	
	Control	−0.0692	
Left frontal lobe	AD	−0.000333	*5.98×10^{-6} (20.7)
	MCI	−0.0722	
	Control	−0.0599	
Right frontal lobe	AD	−0.0269	*0.001 (9.2)
	MCI	−0.0917	
	Control	−0.0626	
Left parietal lobe	AD	−0.00832	0.070 (2.9)
	MCI	−0.0383	
	Control	−0.0479	
Right parietal lobe	AD	−0.0149	0.074 (2.9)
	MCI	−0.0668	
	Control	−0.0503	

*p values showing a significant difference in mean slope across groups for given brain region.

Table 2. Multiple comparisons across clinical phenotypes for regions with significantly different glymphatic rates

Brain region	Phenotype 1	Phenotype 2	Mean slope difference	p value	Reject null
Left temporal lobe	AD	Control	−0.0417	0.004	*True
	AD	MCI	−0.0334	0.157	False
	Control	MCI	0.0083	0.8	False
Right temporal lobe	AD	Control	−0.0624	0.0015	*True
	AD	MCI	−0.0558	0.0649	False
	Control	MCI	0.0066	0.9	False
Left frontal lobe	AD	Control	−0.0597	0.001	*True
	AD	MCI	−0.0719	0.001	*True
	Control	MCI	−0.0122	0.614	False
Right frontal lobe	AD	Control	−0.0356	0.008	*True
	AD	MCI	−0.0648	0.001	*True
	Control	MCI	−0.0291	0.121	False

AD, Alzheimer's Dementia; MCI, mild cognitive impairment.
*p values indicating significant differences lie between mean slopes for given phenotypes.

Case Rep Neurol 2023;15:177–186
DOI: 10.1159/000530980

Table 3. Summary of glymphatic clearance results for the three subjects

Year	L temp slope	R temp slope	L frontal slope	R frontal slope	L parietal slope	R parietal slope	MMSE score
Subject 1							
Nov 2019	−0.036	−0.0722	−0.0789	−0.1282	−0.0638	−0.0632	30/30
April 2021	−0.0255	−0.0055	−0.0036	−0.0815	−0.1102	−0.1235	28/30
Percent change from 2019	43% decline clearance	92% decline clearance	95% decline clearance	21% decline clearance	94% increase clearance	74% increase clearance	
May 2021	−0.0191	−0.0315	−0.0128	−0.0194	−0.0745	−0.093	N.D.
Percent change from 2019	42% decline clearance	56% decline clearance	84% decline clearance	85% decline clearance	11% increase clearance	58% increase clearance	
Subject 2							
July 2021	−0.00611	−0.0045	−0.0195	−0.0158	−0.0005	−0.0282	15/30
Range of values c/w AD group	Within AD range of clearance-Pilot study	Within AD range of clearance-Pilot study	Within AD range of clearance-Pilot study	Within AD range of clearance-Pilot study	Within AD range of clearance-Pilot study	Outside AD clearance range-Pilot study	
Subject 3							
Dec 2021	−0.0611	−0.0437	−0.082	−0.072	−0.0326	−0.0845	27/30
June 2022	−0.053	−0.0717	−0.0558	−0.0749	−0.0186	−0.0526	28/30
Percent change from 2021	0.2% Decline clearance	6% Increase clearance	32% Decline clearance	4.1% Decline clearance	44% Decline clearance	26% Decline clearance	

Normal ranges of clearance rates from the pilot study: **temporal lobe** Nl < −0.05; **frontal lobe** Nl < −0.05; **parietal lobe** < −0.05 Note: Increased slope negativity the more efficient the glymphatic clearance.

These findings suggest that ASL measurement of residual labeled proton clearance may allow for effectively detecting progression of MCI to AD as found in participant 1. The degree of deterioration in glymphatic clearance over time in participant 1 exceeded their anticipated cognitive decline by MMSE and spousal assessment. This suggests BBB breakdown, dysfunction of glymphatic clearance and reduced capillary transit times are upstream events predating neuronal loss. We note typical AD cognitive changes and MMSE scores with markedly reduced glymphatic clearance in participant 2 which recapitulates findings from our earlier study [18].

Participant 3's reduction in parietal clearance time despite a stable clinical appearance suggests that the physiologic changes predate the cognitive decline and as such, may provide a sensitive marker for identification of early progression useful for clinical trials investigating disease modifying treatments at early stage AD.

Of further interest is the increased biparietal glymphatic clearance rate in participant 1 in the follow-up studies compared with the first, suggesting compensatory shift of vascular autoregulation to unaffected cortex associated with decline of clearance in the bitemporal and bi-frontal lobes. This ASL technique indirectly demonstrates the progressive BBB leak and pathophysiologic changes in cMTT and/or glymphatic flow present in the early MCI phase of neurodegenerative disease in this small sample. The reduced

cMTT is well recognized in AD, as opposed to prolonged arterial mean transit times which have been shown to be normal in AD [22]. Prolonged capillary transit times have been described in AD which likely results from the EC dysfunction causing BBB leak contributing to reduced rate of proton clearance [1, 23, 24]. Most of the signal from the labeled blood rapidly exits the cerebrum via the vascular route within 3–3.5 s. Any signal remaining has likely entered the interstitial space which in the case of an intact glymphatic system will clear more slowly and the rate of clearance determined with multiple late post-labeling inversions. If there is, however, substantial leak of labeled protons into the interstitium and/or if dysfunction of the glymphatic system is present, then substantial reduction in rate of clearance will be present [18, 19, 24, 25]. Separating glymphatic clearance reduction from prolonged capillary transit times is not possible by this technique and is likely a moot distinction, as it is the reduction in clearance of labeled protons itself, regardless of source, that is of interest and correlated with progression to AD.

Limitations of this study include a small sample size and low residual signal present in the long inversion times used. Sampling error given the hand-drawn regions of interest is an additional source or error. The latter was reduced by choosing a standard sampling size for each brain region large enough to maximize the quantity of pixels averaged without including subarachnoid or ventricular spaces that would introduce error. Likewise including 7 data points in the slope determination better defines the clearance rate. The technique does not distinguish between prolonged cMTT and leaked or trapped interstitial labeled protons. However, the reduced clearance rate infers one or both are present and develop in preclinical AD as a consequence of BBB leak. Availability of a segmentation tool would both improve efficiency of post-processing and may reduce sampling error. Other 3D ASL techniques may further improve scan time efficiency and post processing efficiency. Hippocampal volume loss and APOE 4 status were not assessed in this study and are a study limitation.

The results of this study suggest potential for further development of this approach in differentiating MCI transition to AD. By design, it captures the early pathophysiologic changes of reduced cMTT/glymphatic clearance. A larger prospective study is necessary to validate this approach. Most community based 3T magnets have commercially available 3D ASL sequences in software packages making this a simple, noninvasive, and time efficient add-on to MRI investigation of MCI/dementia.

Future efforts at pharmacologic intervention targeting these early changes present a major novel focus in mitigating neurodegenerative disease before the tragic consequences develop. This ASL-MRI approach with further development may provide the needed non-invasive tool to screen and treat at-risk patients in the preclinical state [26, 27]. Finally, this approach is noninvasive, time efficient, inexpensive, and commercially available on 3T magnets making it amenable for broad adoption.

Acknowledgments

We wish to acknowledge the following former and present students, and faculty who have participated in data collection and without whose help and dedication this project would not have been possible Kevin Daniel Thomas DO, Kyle Drury DO, Lilian Yin Ni Lee DO, Logan Stern DO, Yoshua Mathai, DO, Mathew Wend, DO, Emma Neahusan, DO, Rebekah Tanas, DO, Samantha Jo Scarola DO, Sriharsha Ponna DO, Carson Luke Williams DO, Zachary Gross DO, Bradley Waman Clark BS, Emilee R Welton BS, Seung Yoon Lee DO, David Truitte MD, and Jeff Jaspers PhD. The authors would also like to express our gratitude to the physicians at CVFP for participant referrals, and CENTRA health for providing MRI research time availability.

Statement of Ethics

This study protocol was reviewed and approved by the CENTRA Health Institutional Review Board (IRB # CHIRB0452). Written informed consent was obtained from the patients and in the case of the participants with AD from both the participant and their POA for publication of this case report and any accompanying images. No identifying information is included in the manuscript and is otherwise securely held. Consent to publish was granted by Liberty University College of Osteopathic Medicine.

Conflict of Interest Statement

Nicholas L. Rider, DO receives funding from the NIH (unrelated to this study) as well as from the Jefferey Modell Foundation and Takeda Pharmaceuticals. He receives consulting fees from Pharming Healthcare, Takeda Pharmaceuticals, and royalties from Wolters Kluwer. The other authors, Charles R. Joseph, Alec Kreilach, Victoria Ashley Reyna, Thomas Ashton Kepler, Brittany Viola Taylor, Jubin Kang, and Dallas McCorkle have no conflicts of interest to declare.

Funding Sources

Funding was provided by Liberty University College of Osteopathic Medicine intramural grant #2019-03.

Author Contributions

Charles R. Joseph: methodological conception, data collection and analysis, manuscript preparation and review. Corresponding author Alec Kreilach: data collection and manuscript preparation and review. Victoria Ashley Reyna, Thomas Ashton Kepler, Brittany Viola Taylor Jubin Kang, and Dallas McCorkle: data collection and manuscript preparation. Nicholas L. Rider: data collection, manuscript preparation, and statistical analysis.

Data Availability Statement

All data generated or analyzed during this study are included in this article and its online supplementary material. Further inquiries can be directed to the corresponding author.

References

1 Propson NE, Roy ER, Litvinchuk A, Köhl J, Zheng H. Endothelial C3a receptor mediates vascular inflammation and blood-brain barrier permeability during aging. J Clin Invest. 2021;131(1):e140966.
2 Barisano G, Montagne A, Kisler K, Schneider JA, Wardlaw JM, Zlokovic BV. Blood-brain barrier link to human cognitive impairment and Alzheimer's Disease. Nat Cardiovasc Res. 2022 Feb;1(2):108–15.
3 Bhatia K, Ahmad S, Kindelin A, Ducruet AF. Complement C3a receptor-mediated vascular dysfunction: a complex interplay between aging and neurodegeneration. J Clin Invest. 2021;131(1):e144348.
4 Singh, R; Pharmacology, A. S.-A. J. of P. and, & 2020; Asian Journal Of Pharmacy and Pharmacology. Involvement of neuroinflammatory mediators in the pathogenesis of neurodegeneration. Ajpp; 2020.
5 Zlokovic BV. The blood-brain barrier in health and chronic neurodegenerative disorders. Neuron. 2008;57(2):178–201.

6 Montagne A, Barnes S, Sweeney M, Neuron MH. Neuron, Blood-brain barrier breakdown in the aging human hippocampus. Elsevier; 2015. Retrieved from https://www.sciencedirect.com/science/article/pii/S0896627314011416.
7 Fisher RA, Miners JS, Love S. Pathological changes within the cerebral vasculature in Alzheimer's disease: new perspectives. Brain Pathol. 2022;32(6):e13061.
8 Lin Z, Sur S, Liu P, Li Y, Jiang D, Hou X, et al. Blood–brain barrier breakdown in relationship to Alzheimer and vascular disease. Ann Neurol. 2021;90(2):227–38.
9 Nehra G, Bauer B, Hartz AMS. Blood-brain barrier leakage in Alzheimer's disease: from discovery to clinical relevance. Pharmacol Ther. 2022;234:108119.
10 Natale G, Limanaqi F, Busceti CL, Mastroiacovo F, Nicoletti F, Puglisi-Allegra S, et al. Glymphatic system as a gateway to connect neurodegeneration from periphery to CNS. Front Neurosci. 2021;15:639140.
11 Ittner LM, Götz J. Amyloid-β and tau: a toxic pas de deux in Alzheimer's disease. Nat Rev Neurosci. 2011;12(2):65–72.
12 Ujiie M, Dickstein DL, Carlow DA, Jefferies WA. Blood-brain barrier permeability precedes senile plaque formation in an alzheimer disease model. Microcirculation. 2003;10(6):463–70.
13 Lendahl U, Nilsson P, Betsholtz C. Emerging links between cerebrovascular and neurodegenerative diseases: a special role for pericytes. EMBO Rep. 2019;20(11):e48070.
14 Zhao A, Li Y, Yan Y, Qiu Y, Li B, Xu W, et al. Increased prediction value of biomarker combinations for the conversion of mild cognitive impairment to Alzheimer's dementia. Transl Neurodegener. 2020;9(1):30.
15 Montagne A, Barnes SR, Nation DA, Kisler K, Toga AW, Zlokovic BV. Imaging subtle leaks in the blood–brain barrier in the aging human brain: potential pitfalls, challenges, and possible solutions. Geroscience. 2022 Jun;44(3):1339–51.
16 Joseph, CR. Novel MRI techniques identifying vascular leak and paravascular flow reduction in early alzheimer disease. Biomedicines. 2020;8(7):228.
17 Huang D, Guo Y, Guan X, Pan L, Zhu Z, Chen Z, et al. Recent advances in arterial spin labeling perfusion MRI in patients with vascular cognitive impairment. J Cereb Blood Flow Metab. 2023 Feb;43(2):173–84.
18 Joseph CR, Benhatzel CM, Stern LJ, Hopper OM, Lockwood MD. Pilot study utilizing MRI 3D TGSE PASL (arterial spin labeling) differentiating clearance rates of labeled protons in the CNS of patients with early Alzheimer disease from normal subjects. Magn Reson Mater Phys Biol Med. 2020;33(4):559–68.
19 Li KL, Zhu X, Hylton N, Jahng GH, Weiner MW, Schuff N. Four-phase single-capillary stepwise model for kinetics in arterial spin labeling MRI. Magn Reson Med. 2005;53(3):511–8.
20 Günther M, Oshio K, Feinberg DA. Single-shot 3D imaging techniques improve arterial spin labeling perfusion measurements. Magn Reson Med. 2005;54(2):491–8.
21 Alsop DC, Detre JA, Golay X, Günther M, Hendrikse J, Hernandez-Garcia L, et al. Recommended implementation of arterial spin-labeled perfusion MRI for clinical applications: a consensus of the ISMRM perfusion study group and the European consortium for ASL in dementia. Magn Reson Med. 2015;73(1):102–16.
22 Fernández-Seara MA, Wang Z, Wang J, Rao H-Y, Guenther M, Feinberg DA, et al. Continuous arterial spin labeling perfusion measurements using single shot 3D GRASE at 3 T. Magn Reson Med. 2005;54(5):1241–7.
23 Yoshiura T, Hiwatashi A, Yamashita K, Ohyagi Y, Monji A, Takayama Y, et al. Simultaneous measurement of arterial transit time, arterial blood volume, and cerebral blood flow using arterial spin-labeling in patients with alzheimer disease. AJNR Am J Neuroradiol. 2009;30(7):1388–93.
24 Eskildsen SF, Gyldensted L, Nagenthiraja K, Nielsen RB, Hansen MB, Dalby RB, et al. Increased cortical capillary transit time heterogeneity in Alzheimer's disease: a DSC-MRI perfusion study. Neurobiol Aging. 2017;50:107–18.
25 Liu Y, Zhu X, Feinberg D, Guenther M, Gregori J, Weiner MW, et al. Arterial spin labeling MRI study of age and gender effects on brain perfusion hemodynamics. Magn Reson Med. 2012;68(3):912–22.
26 de Oliveira Silva F, Ferreira JV, Plácido J, Sant'Anna P, Araújo J, Marinho V, et al. Three months of multimodal training contributes to mobility and executive function in elderly individuals with mild cognitive impairment, but not in those with Alzheimer's disease: a randomized controlled trial. Maturitas. 2019;126:28–33.
27 Rye I, Vik A, Kocinski M, LundervoldAS, Lundervold AJ. Predicting conversion to Alzheimer's disease in individuals with Mild Cognitive Impairment using clinically transferable features. Sci Rep. 2022 Sep 16;12(1):15566.